J|A|C|S COMMUNICATIONS

Published on Web 12/30/2009

Porous Phosphorescent Coordination Polymers for Oxygen Sensing

Zhigang Xie, Liqing Ma, Kathryn E. deKrafft, Athena Jin, and Wenbin Lin*

Department of Chemistry, CB#3290, University of North Carolina, Chapel Hill, North Carolina 27599

Received November 12, 2009; E-mail: wlin@unc.edu

Coordination polymers represent a new class of tunable materials that have shown great promise in a number of applications, including gas storage,[1] catalysis,[2] nonlinear optics,[3] and nanomedicine.[4] Because of their propensity to exhibit high porosity, coordination polymers provide an interesting platform for probing the interactions between the frameworks and gaseous molecules. A large number of luminescent coordination polymers have appeared in the literature over the past decade,[5] either by taking advantage of the intrinsic fluorescent property of the organic bridging ligands or the luminescent property of a lanthanide metal ion (such as Eu^{3+} or Tb^{3+}).[6] The luminescent properties of porous coordination polymers can be perturbed by a small molecule or ion, thereby providing an effective means for chemical sensing. Recently, a microporous fluorescent coordination polymer was shown to reversibly detect high explosives in the gas phase,[7] whereas lanthanide-based luminescent coordination polymers were shown to respond to the presence of a metal ion or an anion in solution.[8] Cyclometalated Ir complexes such as $Ir(ppy)_3$ (where ppy is 2-phenylpyridine) are highly efficient phosphorescent molecules owing to the facile intersystem crossing to populate the ^{3}MLCT states, and have been extensively used in light-emitting devices.[9] The ^{3}MLCT phosphorescence can be readily quenched by molecules with a triplet ground state, thereby providing accurate sensing for oxygen.[10] We hypothesized that $Ir(ppy)_3$ derivatives can be incorporated into coordination polymers to lead to highly phosphorescent materials as chemical sensors. Herein we report the design and synthesis of highly phosphorescent coordination polymers based on $Ir(ppy)_3$ derivatives and their application in oxygen sensing via luminescence quenching.

Scheme 1

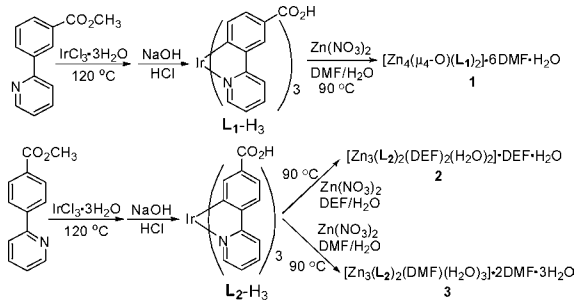

$Ir(ppy)_3$ derivatives, $\mathbf{L_1}$-H_3 and $\mathbf{L_2}$-H_3, each containing three carboxylic acid groups, were synthesized by microwave heating of $IrCl_3 \cdot 3H_2O$ and methyl 3-(2-pyridyl)benzoate or methyl 4-(2-pyridyl)benzoate at 120 °C, followed by base-catalyzed hydrolysis (Scheme 1). Reactions of $Zn(NO_3)_2 \cdot 6H_2O$ with $\mathbf{L_1}$-H_3 in dimethylformamide (DMF)/H_2O at 90 °C for 24 h afforded single crystals of $[Zn_4(\mu_4\text{-}O)(\mathbf{L_1})_2] \cdot 6DMF \cdot H_2O$ (**1**).[11] Similar reactions of $Zn(NO_3)_2 \cdot 6H_2O$ and $\mathbf{L_2}$-H_3 in diethylformamide (DEF)/H_2O or DMF/H_2O resulted in single crystals of $[Zn_3(\mathbf{L_2})_2(DEF)_2(H_2O)_2] \cdot DEF \cdot H_2O$ (**2**) or $[Zn_3(\mathbf{L_2})_2(DMF)(H_2O)_3] \cdot 2DMF \cdot 3H_2O$ (**3**), respectively. Compound **1** crystallizes in the trigonal $R\bar{3}$ space group with one-third of an $\mathbf{L_1}$ ligand, two-thirds of a Zn center, one-sixth of a μ_4-O atom, one DMF, and one-sixth of a water molecule in the asymmetric unit. The Ir center in the $\mathbf{L_1}$ ligand adopts a *fac* coordination geometry due to the strong *trans* effect of the Ir−C bond, leading to a cone arrangement of the three carboxylate groups (Figure 1a). The carboxylate groups from six adjacent $\mathbf{L_1}$ ligands coordinate to four Zn centers to form $[Zn_4(\mu_4\text{-}O)(carboxylate)_6]$ secondary building units (SBUs) which link $\mathbf{L_1}$ ligands to form two-dimensional (2D) bilayers of $[Zn_4(\mu_4\text{-}O)(\mathbf{L_1})_2]$ (Figure 1b), which pack along the *c*-axis with a closest interlayer distance of 3.6 Å. **1** possesses open channels of 7.9 Å × 4.3 Å that are perpendicular to the (1, −1, 6) plane (Figure 1c) and contain guest solvent molecules. Thermogravimetric analysis (TGA) of **1** showed 64.5% weight loss due to solvents and ligands from rt to 600 °C (calcd 66.5%).

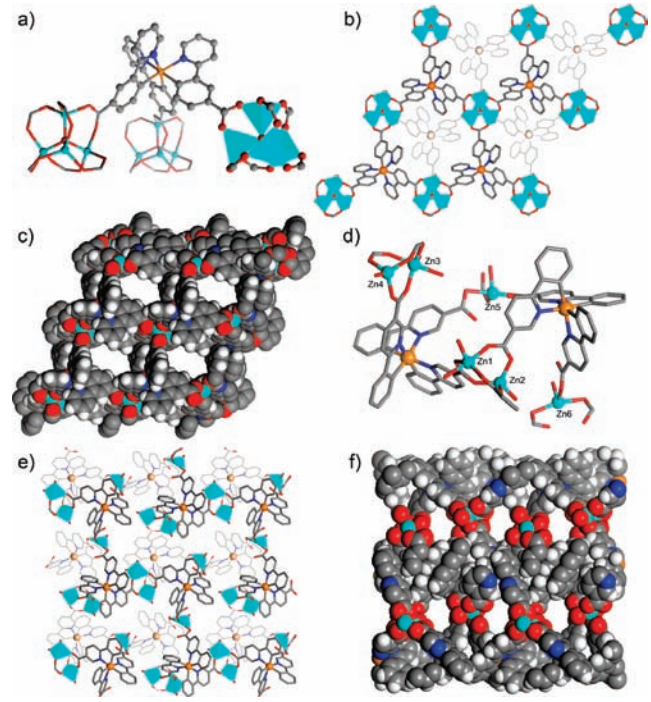

Figure 1. X-ray structures for **1** and **2**. (a) Ball-stick/polyhedra model showing the connectivity of $\mathbf{L_1}$ and $[Zn_4O(carboxylate)_6]$ SBUs. (b) A top view of the 2D bilayer structure of **1**. (c) Space-filling model of **1** viewed perpendicular to the (1,−1, 6) plane. (d) Ball-stick model showing the connetctivity of $\mathbf{L_2}$ and Zn ions in **2**. (e) Top view of the 2D bilayer structure of **2**. (f) Space-filling model of **2** as viewed down the *b*-axis.

2 crystallizes in the triclinic $P\bar{1}$ space group with six Zn centers and four $\mathbf{L_2}$ ligands in the asymmetric unit. The three carboxylate groups in the $\mathbf{L_2}$ ligand adopt a narrower cone configuration than that of **1** due to their placement on the 5-positions of the ppy moieties (Figure 1d). As a result, **2** adopts a different structure from **1** and contains both mononuclear and dinuclear Zn connecting points. The Zn1/Zn2 and Zn3/Zn4 centers are bridged by three carboxylates. Zn2

10.1021/ja909629f

and Zn3 adopt a distorted trigonal bipyramid geometry by coordinating to two DEF molecules, whereas Zn1 and Zn4 adopt a tetrahedral geometry by coordinating to an H_2O molecule. Zn5 and Zn6 coordinate to three monodentate carboxylates and one H_2O molecule to adopt a distorted trigonal bipyramid geometry. The $\mathbf{L_2}$ ligands are linked by these Zn connecting points to form 2D bilayers that pack along the *a*-axis, with the largest channels of 4 Å × 3 Å running along the *b*-axis. The structure of **3** is similar to that of **2** with the exception of different coordinating solvent molecules. TGA of **2** and **3** showed 65.7% (calcd 67.3%) and 62.6% (calcd 66.9%) solvent and ligand weight loss from rt to 600 °C, respectively.

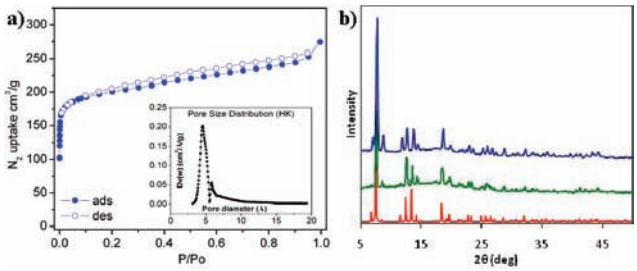

Figure 2. (a) N_2 adsorption isotherm of **1** at 77 K. (Inset) HK pore size distribution. (b) PXRD patterns of **1**: red, simulated; green, pristine solid; blue, desolvated solid.

The permanent porosity of **1** is shown by N_2 adsorption at 77 K and CO_2 adsorption at 273 K. Type I isotherms were obtained for **1**, indicating its microporous structure with a nitrogen BET surface area of 764 m^2/g and a bimodal pore size (calcd by the HK method) distribution centering at 4.5 and 5.8 Å (Figure 2a). **1** exhibits a BET surface area of 958 m^2/g based on CO_2 adsorption. The framework stability of **1** was supported by a perfect match between powder X-ray diffraction (PXRD) patterns of pristine **1** and desolvated **1** (Figure 2b). In contrast, there is no N_2 uptake for **2** or **3** under the same conditions, indicating their nonporous nature. The PXRD pattern of desolvated **2** is different from that of pristine **2**, indicating framework distortion during the desolvation process. These results underscore the role of rigid SBUs in reinforcing the framework stability in coordination polymers.

Experiments were conducted to determine the luminescence quenching of the Ir-containing coordination polymers by oxygen. Detailed photophysical data of the new $Ir(ppy)_3$ derivatives and their coordination polymers are shown in Figures S6−8, Supporting Information (SI). Desolvated crystal samples of **1**−**3** were each ground and pressed onto the surface of a transparent KBr pellet, which was placed in a quartz cuvette equipped with a vacuum/O_2 port.[12] An excitation wavelength of 385 nm was used for $\mathbf{L_1}$-H_3, **1**, and **3**, and 400 nm was used for $\mathbf{L_2}$-H_3 and **2**. Emission was detected at 538 nm for $\mathbf{L_1}$-H_3, **1**, and **3**, and at 565 nm for $\mathbf{L_2}$-H_3 and **2**. The cuvette was subjected to dynamic vacuum for 2 h before gradually dosing in O_2 from 0.05 to 1.0 atm. The luminescence intensity was measured for 30 s after each dose. At 1 atm O_2, the quenching efficiencies for **1**, **2**, **3**, $\mathbf{L_1}$-H_3, and $\mathbf{L_2}$-H_3 are 59%, 41%, 32%, 16%, and 8%, respectively. The luminescence intensity of **1** dropped to a stable value instantly after each dose of O_2 to give a linear Stern−Volmer plot (I_0/I vs P_{O_2}) as shown in Figure 3a. Luminescence measurements after alternating cycles of O_2 dosing at 0.1 atm (30 s) and O_2 removal under vacuum (120 s) indicated that the luminescence of **1** is reversibly quenched by O_2, with <5% of the original luminescence lost after eight cycles (Figure 3b). In contrast, gradual decreases in luminescence intensity were observed for **2**, **3**, $\mathbf{L_1}$-H_3, and $\mathbf{L_2}$-H_3 during each 30 s period, and the O_2 quenching behaviors are irreversible. **2** and **3** show some luminescence quenching because O_2 has access to the Ir sites on the surface and in the incompletely obstructed pores in the collapsed framework. However, it takes much longer to remove O_2 from these distorted pores. Ir-containing coordination polymers thus need to be permanently porous for their luminescence to be effectively and reversibly quenched by O_2, owing to the need for rapid diffusion of O_2 through the open channels.

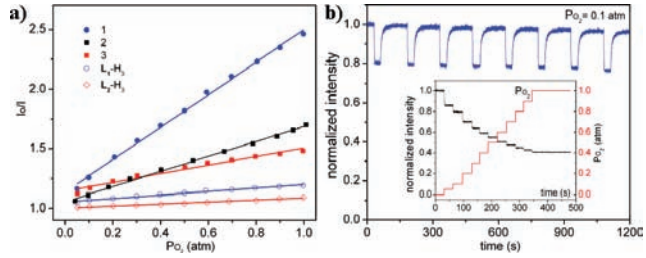

Figure 3. (a) Stern−Volmer plot showing I_0/I vs O_2 partial pressure for Ir-complexes $\mathbf{L_1}$-H_3 and $\mathbf{L_2}$-H_3 and coordination polymers **1**−**3**. (b) Reversible quenching of phosphorescence of **1** upon alternating exposure to 0.1 atm O_2 and application of vacuum. The inset shows rapid equilibration of phosphorescence of **1** after each dose of O_2.

In summary, we have designed and synthesized highly porous and phosphorescent Ir-containing coordination polymers and demonstrated oxygen sensing via efficient and reversible luminescence quenching. The tunability of coordination polymers should allow for the extension of this strategy to the design of sensory materials for other important analytes.

Acknowledgment. We thank DOE (DE-SC0001011) and NSF (DMR-0906662) for financial support.

Supporting Information Available: Experimental procedures and characterization data. This material is available free of charge via the Internet at http://pubs.acs.org.

References

(1) (a) Rowsell, J. L. C.; Yaghi, O. M. *Angew. Chem., Int. Ed.* **2005**, *44*, 4670. (b) Mircea, D.; Long, J. R. *Angew. Chem., Int. Ed.* **2008**, *47*, 6766–6779. (c) Kesanli, B.; Cui, Y.; Smith, M.; Bittner, E.; Bockrath, B.; Lin, W. *Angew. Chem., Int. Ed.* **2005**, *44*, 72.
(2) (a) Ma, L.; Abney, C.; Lin, W. *Chem. Soc. Rev.* **2009**, *38*, 1248–1256. (b) Lee, J.; Farha, O. K.; Roberts, J.; Scheidt, K. A.; Nguyen, S. T.; Hupp, J. T. *Chem. Soc. Rev.* **2009**, *38*, 1450.
(3) Evans, O. R.; Lin, W. *Acc. Chem. Res.* **2002**, *35*, 511.
(4) Lin, W.; Rieter, W. J.; Taylor, K. M. L. *Angew. Chem., Int. Ed.* **2009**, *48*, 650–658.
(5) Allendorf, M. D.; Bauer, C. A.; Bhakta, R. K.; Houk, R. J. T. *Chem. Soc. Rev.* **2009**, *38*, 1330–1352.
(6) (a) Ma, L.; Evans, O. R.; Foxman, B. M.; Lin, W. *Inorg. Chem.* **1999**, *38*, 5837–5840. (b) Rieter, W. J.; Taylor, K. M. L.; An, H.; Lin, W.; Lin, W. *J. Am. Chem. Soc.* **2006**, *128*, 9024–9025. (c) Cahill, C. L.; de Lill, D. T.; Frisch, M. *CrystEngComm* **2007**, *9*, 15–26. (d) Wang, P.; Ma, J.-P.; Dong, Y.-B.; Huang, R.-Q. *J. Am. Chem. Soc.* **2007**, *129*, 10620.
(7) Lan, A.; Li, K.; Wu, H.; Olson, D. H.; Emge, T. J.; Ki, W.; Hong, M.; Li, J. *Angew. Chem., Int. Ed.* **2009**, *48*, 2334–2338.
(8) (a) Chen, B.; Wang, L.; Xiao, Y.; Fronczek, F. R.; Xue, M.; Cui, Y.; Qian, G. *Angew. Chem., Int. Ed.* **2009**, *48*, 500–503. (b) Chen, B.; Wang, L.; Zapata, F.; Qian, G.; Lobkovsky, E. B. *J. Am. Chem. Soc.* **2008**, *130*, 6718–6719.
(9) (a) Gong, X.; Ostrowski, J. C.; Bazan, G. C.; Moses, D.; Heeger, A. J.; Liu, M. S.; Jen, A. K. Y. *Adv. Mater.* **2003**, *15*, 258. (b) Thompson, M. E. *MRS Bull.* **2007**, *32*, 694–701.
(10) (a) Mak, C. S. K.; Pentlehner, D.; Stich, M.; Wolfbeis, O. S.; Chan, W. K.; Yersin, H. *Chem. Mater.* **2009**, *21*, 2173–2175. (b) DeRosa, M. C.; Hodgson, D. J.; Enright, G. D.; Dawson, B.; Evans, C. E. B.; Crutchley, R. *J. Am. Chem. Soc.* **2004**, *126*, 7619–7626.
(11) Several examples of mixed metal−organic frameworks are known. (a) Chen, B.; Zhao, X.; Putkham, A.; Hong, K.; Lobkovsky, E. B.; Hurtade, E. J.; Fletcher, A. J.; Thomas, K. M. *J. Am. Chem. Soc.* **2008**, *130*, 6411–6423. (b) Cho, S.-H.; Ma, B.; Nguyen, S. T.; Hupp, J. T.; Albrecht-Schmitt, T. E. *Chem. Commun.* **2006**, 2563–2565.
(12) The pellet was angled at 135° towards the excitation beam so that the direct reflections would travel in the opposite direction of the detector in order to minimize the scattering effect.

JA909629F